
Divide-and-Conquer Predictive Coding: a Structured Bayesian Inference Algorithm

Anonymous Author(s)

Affiliation

Address

email

Abstract

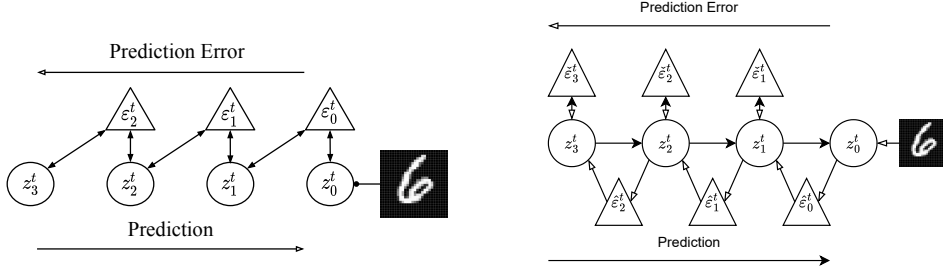
1 Unexpected stimuli induce “error” or “surprise” signals in the brain. The theory
2 of predictive coding promises to explain these observations in terms of Bayesian
3 inference by suggesting that the cortex implements variational inference in a proba-
4 bilistic graphical model. However, when applied to machine learning tasks, this
5 family of algorithms has yet to perform on par with other variational approaches in
6 high-dimensional, structured inference problems. To address this, we introduce a
7 novel predictive coding algorithm for structured generative models, that we call
8 divide-and-conquer predictive coding (DCPC). DCPC differs from other formula-
9 tions of predictive coding, as it respects the correlation structure of the generative
10 model and provably performs maximum-likelihood updates of model parameters,
11 all without sacrificing biological plausibility. Empirically, DCPC achieves better
12 numerical performance than competing algorithms and provides accurate inference
13 in a number of problems not previously addressed with predictive coding. We
14 provide an open implementation of DCPC in Pyro on Github.

15 1 Introduction

16 In recent decades, the fields of cognitive science, machine learning, and theoretical neuroscience have
17 borne witness to a flowering of successes in modeling intelligent behavior via statistical learning.
18 Each of these fields has taken a different approach: cognitive science has studied probabilistic
19 *inverse inference* [Chater et al., 2006, Pouget et al., 2013, Lake et al., 2017] in models of each task
20 and environment, machine learning has employed the backpropagation of errors [Rumelhart et al.,
21 1986, Lecun et al., 2015, Schmidhuber, 2015], and neuroscience has hypothesized that *predictive*
22 *coding* [Srinivasan et al., 1982, Rao and Ballard, 1999, Friston, 2005, Bastos et al., 2012, Spratling,
23 2017, Hutchinson and Barrett, 2019, Millidge et al., 2021] (PC) may explain neural activity in
24 perceptual tasks. These approaches share in common a commitment to “deep” models, in which task
25 processing emerges from the composition of elementary units.

26 At the computational level, probabilistic theories of perception suggest that the brain is an hypothesis
27 testing machine, where the world is perceived via Bayesian inference [Doya, 2007]. In the PC
28 framework, hypotheses correspond to prediction signals that flow down the cortical hierarchy to inhibit
29 the bottom-up processing of predictable (or irrelevant) stimuli. Combining these top-down predictions
30 with a bottom-up stimulus signal generates prediction errors, defined as the (weighted) difference
31 between predicted and actual signals [Hoemann et al., 2017, Barrett, 2022]. Algorithmically, PC
32 implements variational inference [Friston et al., 2006]: under some specific assumptions, a prediction
33 error ε is the gradient of a variational free energy defined over a hierarchical Gaussian generative
34 model, i.e., $\varepsilon := \nabla_{\mu} \log \mathcal{N}(\mu, \tau) = \tau(x - \mu)$, with respect to the location parameter μ , of a Gaussian
35 $x \sim \mathcal{N}(\mu, \tau)$ log-density parameterized by mean μ and precision τ .

36 In machine learning, predictive coding algorithms have recently gained popularity for their theoretical
37 potential to provide a more biologically plausible alternative to backpropagation for training neural



(a) Classical PC learns a mean-field approximate posterior with prediction error layers. (b) Divide-and-conquer PC approximates the joint posterior with bottom-up and recurrent errors.

Figure 1: Where classical predictive coding has layers communicate through shared error units, divide-and-conquer predictive coding separates recurrent from “bottom-up” error pathways to target complete conditional distributions rather than posterior marginal distributions.

networks [Salvatori et al., 2023, Song et al., 2024]. However, PC does not perform comparably in these tasks to backpropagation due to limitations in current formulations. First, predictive coding for gradient calculation typically models every node in the computation graph with a Gaussian, and hence fails to express many common generative models. Recent work on PC has addressed this by allowing approximating non-Gaussian energy functions with samples [Pinchetti et al., 2022]. Second, the Laplace approximation to the posterior infers only a maximum-a-posteriori (MAP) estimate and Gaussian covariance for each latent variable, keeping PC from capturing multimodal or correlated distributions. Third, this loose approximation to the posterior distribution results in inaccurate, high-variance updates to the generative model’s parameters.

In this work we propose a new algorithm, *divide-and-conquer predictive coding* (DCPC), for approximating structured target distributions with populations of Monte Carlo samples. DCPC goes beyond Gaussian assumptions, and decomposes the problem of sampling from structured targets into local coordinate updates to individual random variables. These local updates are informed by unadjusted Langevin proposals parameterized in terms of biologically plausible prediction errors. Nesting the local updates within divide-and-conquer Sequential Monte Carlo [Lindsten et al., 2017, Kuntz et al., 2024] ensures that DCPC can target any statically structured graphical model, while Theorem 2 provides a locally factorized way to learn model parameters by maximum marginal likelihood.

DCPC also provides a computational perspective on the canonical cortical microcircuit [Bastos et al., 2012, 2020, Campagnola et al., 2022] hypothesis in neuroscience. Experiments have suggested that deep laminar layers in the cortical microcircuit represent sensory imagery, while superficial laminar represent raw stimulus information [Bergmann et al., 2024]; experiments in a predictive coding paradigm specifically suggested that the deep layers represent “predictions” while the shallow layers represent “prediction errors”. This circuitry could provide the brain with its fast, scalable, generic Bayesian inference capabilities. Figure 1 compares the computational structure of DCPC with that of previous PC models. The following sections detail this work’s contributions:

- Section 3 defines the divide-and-conquer predictive coding algorithm and shows how to use it as a variational inference algorithm;
- Section 4 examines under what assumptions the cortex could plausibly implement DCPC, proving two theorems that contribute to biological plausibility;
- Section 5 demonstrates DCPC experimentally in head-to-head comparisons against recent generative models and inference algorithms from the predictive coding literature.

Section 2 will review the background for Section 3’s algorithm: the problem predictive coding aims to solve and a line of recent work addressing that problem from which this paper draws.

2 Background

This section reviews the background necessary to construct the divide-and-conquer predictive coding algorithm in Section 3. Let us assume we have a directed, acyclic graphical model with a joint density

split into observations $x \in \mathbf{x}$ and latents $z \in \mathbf{z}$, parameterized by some θ at each conditional density

$$p_\theta(\mathbf{x}, \mathbf{z}) := \prod_{x \in \mathbf{x}} p_\theta(x \mid \text{Pa}(x)) \prod_{z \in \mathbf{z}} p_\theta(z \mid \text{Pa}(z)), \quad (1)$$

where $\text{Pa}(z)$ denotes the parents of the random variable $z \in \mathbf{z}$, while $\text{Ch}(z)$ denotes its children.

Empirical Bayes *Empirical Bayes* consists of jointly estimating, in light of the data, both the parameters θ^* and the Bayesian posterior over the latent variables \mathbf{z} , that is:

$$\theta^* = \arg \max_{\theta} p_\theta(\mathbf{x}) = \arg \max_{\theta} \int_{\mathbf{z} \in \mathbf{Z}} p_\theta(\mathbf{x}, \mathbf{z}) d\mathbf{z}, \quad p_{\theta^*}(\mathbf{z} \mid \mathbf{x}) := \frac{p_{\theta^*}(\mathbf{x}, \mathbf{z})}{p_{\theta^*}(\mathbf{x})}.$$

Typically the marginal and posterior densities have no closed form, so learning and inference algorithms treat the joint distribution as a closed-form *unnormalized* density over the latent variables; its integral then gives the normalizing constant for approximation

$$\gamma_\theta(\mathbf{z}) := p_\theta(\mathbf{x}, \mathbf{z}), \quad Z_\theta := \int_{\mathbf{z} \in \mathbf{Z}} \gamma_\theta(\mathbf{z}) d\mathbf{z} = p_\theta(\mathbf{x}), \quad \pi_\theta(\mathbf{z}) := \frac{\gamma_\theta(\mathbf{z})}{Z_\theta}.$$

Neal and Hinton [1998] reduced empirical Bayes to minimization of the *variational free energy*:

$$\mathcal{F}(\theta, q) := \mathbb{E}_{\mathbf{z} \sim q(\mathbf{z})} \left[-\log \frac{\gamma_\theta(\mathbf{z})}{q(\mathbf{z})} \right] \geq -\log Z(\theta). \quad (2)$$

The ratio of densities in Equation 2 is an example of a *weight* used to approximate a distribution known only up to its normalizing constant. The *proposal* distribution $q(\mathbf{z})$ admits tractable sampling, while the unnormalized *target* density $\gamma_\theta(\mathbf{z})$ admits tractable, pointwise density evaluation.

Predictive Coding Computational neuroscientists now often hypothesize that *predictive coding* (PC) can optimize the above family of objective functionals in a local, neurally plausible way [Millidge et al., 2021, 2023]. More in detail, it is possible to define this class of algorithms as follows:

Definition 1 (Predictive Coding Algorithm). *Consider approximate inference in a model $p_\theta(\mathbf{x}, \mathbf{z})$ using an algorithm \mathcal{A} . Salvatori et al. [2023] calls \mathcal{A} a predictive coding algorithm if and only if:*

1. *It maximizes the model evidence $\log p_\theta(\mathbf{x})$ by minimizing a variational free energy;*
2. *The proposal $q(\mathbf{z}) = \prod_{z \in \mathbf{z}} q(z)$ factorizes via a mean-field approximation; and*
3. *Each proposal factor is a Laplace approximation (i.e. $q_\mu(z) := \mathcal{N}(\mu, \Sigma(\mu))$).*

Particle Algorithms In contrast to predictive coding, particle algorithms approach empirical Bayes problems by setting the proposal to a collection of weighted particles (w^k, \mathbf{z}^k) drawn from a sampling algorithm meeting certain conditions (see Definition 2 in Appendix B). Any proposal meeting these conditions (see Proposition 1 in Appendix B and Naesseth et al. [2015], Stites et al. [2021]) defines a free energy functional, analogous to Equation 2 in upper-bounding the model surprisal:

$$\mathcal{F}(\theta, q) := \mathbb{E}_{w, \mathbf{z} \sim q(w, \mathbf{z})} [-\log w] \implies \mathcal{F}(\theta, q) \geq -\log Z(\theta).$$

This paper builds on the particle gradient descent (PGD) algorithm of Kuntz et al. [2023], that works as follows: At each iteration t , PGD diffuses the particle cloud $q_K(\mathbf{z}) = \frac{1}{K} \sum_{k=1}^K \delta_{\mathbf{z}^k}(\mathbf{z})$ across the target log-density with a learning rate η and independent Gaussian noise; it then updates the parameters θ by ascending the gradient of the log-likelihood, estimated by averaging over the particles. The update rules are then the following:

$$\mathbf{z}^{t+1, k} := \mathbf{z}^{t, k} + \eta \nabla_{\mathbf{z}} \log \gamma_{\theta^t}(\mathbf{z}^{t, k}) + \sqrt{2\eta} \xi^k, \quad (3)$$

$$\theta^{t+1} := \theta^t + \eta \left(\frac{1}{K} \sum_{k=1}^K \nabla_{\theta} \log \gamma_{\theta^t}(\mathbf{z}^{t+1, k}) \right). \quad (4)$$

The above equations target the joint density of an entire graphical model¹. When the prior $p_\theta(\mathbf{z})$ factorizes into many separate conditional densities, achieving high inference performance often

¹Kuntz et al. [2023] also interpreted Equation 3 as an update step along the Wasserstein gradient in the space of probability measures. Appendix C extends this perspective to predictive coding of discrete random variables.

	PC	LPC	MCPC	DCPC (ours)
Generative density	Gaussian	Differentiable	Gaussian	Differentiable
Inference approximation	Laplace	Gaussian	Empirical	Empirical
Posterior conditional structure	\times	\times	\times	\checkmark

Table 1: Comparison of divide-and-conquer predictive coding (DCPC) against other predictive coding algorithms. DCPC provides the greatest flexibility: arbitrary differentiable generative models, an empirical approximation to the posterior, and sampling according to the target’s conditional structure.

requires factorizing the inference network or algorithm into conditionals as well [Webb et al., 2018]. Estimating the gradient of the entire log-joint, as in PGD and amortized inference [Dasgupta et al., 2020, Peters et al., 2024], also requires nonlocal backpropagation. To provide a generic inference algorithm for high-dimensional, structured models using only local computations, Section 3 will apply Equation 3 to sample individual random variables in a joint density, combine the coordinate updates via sequential Monte Carlo, and locally estimate gradients for model parameters via Equation 4.

3 Divide-and-Conquer Predictive Coding

The previous section provided a mathematical toolbox for constructing Monte Carlo algorithms based on gradient updates and a working definition of predictive coding. This section will combine those tools to generalize the above notion of predictive coding, yielding the novel *divide-and-conquer predictive coding* (DCPC) algorithm. Given a causal graphical model, DCPC will approximate the posterior with a population $q(\mathbf{z})$ of K samples, while also learning θ explaining the data. This will require deriving local coordinate updates and then parameterizing them in terms of prediction errors.

Let us assume we again have a causal graphical model $p_\theta(\mathbf{x}, \mathbf{z})$ locally parameterized by θ and factorized (as in Equation 1) into conditional densities for each $x \in \mathbf{x}$ and $z \in \mathbf{z}$. DCPC then requires two hyperparameters: a learning rate $\eta \in \mathbb{R}^+$, and particle count $K \in \mathbb{N}^+$, and is initialized (at $t = 0$) via a population of predictions by ancestor sampling defined as $\mathbf{z}^0 \sim \prod_{z \in \mathbf{z}} p_\theta(z^0 \mid \text{Pa}(z^0))$.

To respect the graphical structure of the generative model with only local computations, DCPC recursively targets each variable’s (unnormalized) *complete conditional* density:

$$\gamma_\theta(z; \mathbf{z}_{\setminus z}) = p_\theta(z \mid \text{Pa}(z)) \prod_{v \in \text{Ch}(z)} p_\theta(v \mid \text{Pa}(v)). \quad (5)$$

We observe that the prediction errors ε_z in classical predictive coding, usually defined as the precision weighted difference between predicted and actual value of a variable, can be seen as the *score function* of a Gaussian, where the score is the gradient with respect to the parameter z of the log-likelihood:

$$\varepsilon_z := \nabla_z \log \mathcal{N}(z, \tau) = \tau(x - z);$$

When given the ground-truth parameter z , the *expected* score function $\mathbb{E}_{x \sim p(x|z)} [\nabla_z \log p(x \mid z)] = 0$ under the likelihood becomes zero, making score functions a good candidate for implementing predictive coding. We therefore define ε_z in DCPC as the complete conditional’s score function

$$\varepsilon_z := \nabla_z \log \gamma_\theta(z; \mathbf{z}_{\setminus z}) = \nabla_z \log p_\theta(z \mid \text{Pa}(z)) + \sum_{v \in \text{Ch}(z)} \nabla_z \log p_\theta(v \mid \text{Pa}(v)). \quad (6)$$

This gradient consists of a sum of local prediction-error terms: one for the local “prior” on z and one for each local “likelihood” of a child variable. Defining the prediction error by a locally computable gradient lets us write Equation 3 in terms of ε_z (Equation 6):

$$q_\eta(z^t \mid \varepsilon_z^t, z^{t-1}) := \mathcal{N}(z^{t-1} + \eta \varepsilon_z^t, 2\eta I_z).$$

The resulting proposal now targets the complete conditional density (Equation 5), simultaneously meeting the informal requirement of Definition 1 for purely local proposal computations while also “dividing and conquering” the sampling problem into lower-dimensional coordinate updates.

DCPC assigns the proposed samples importance weights for the complete conditional density

$$z^t \sim q_\eta(z^t \mid z^{t-1}, \varepsilon_z^t) \quad u_z^t = \frac{\gamma_{\theta^{t-1}}(z^t; \mathbf{z}_{\setminus z})}{q_\eta(z^t \mid z^{t-1}, \varepsilon_z^t)}; \quad (7)$$

Algorithm 1 Divide-and-Conquer Predictive Coding for empirical Bayes

Require: learning rate $\eta \in \mathbb{R}^+$, particle count $K \in \mathbb{N}$, number of sweeps $S \in \mathbb{N}$

Require: initial particle vector \mathbf{z}^0 , initial parameters θ^0 , observations $\mathbf{x} \in \mathcal{X}$

```

1: for  $t \in [1 \dots T]$  do                                ▷ Loop through predictive coding steps
2:   for  $s \in [1 \dots S]$  do                                ▷ Loop through Gibbs sweeps over graphical model
3:     for  $z \in \mathbf{z}$  do                                    ▷ Loop through latent variables in graphical model
4:        $\varepsilon_z \leftarrow \nabla_{\mathbf{z}} \log p_{\theta^{t-1}}(z \mid \text{Pa}(z))$                                 ▷ Local prediction error
5:        $\varepsilon_z \leftarrow \varepsilon_z + \sum_{v \in \text{Ch}(z)} \nabla_{\mathbf{z}} \log p_{\theta^{t-1}}(v \mid \text{Pa}(v))$                                 ▷ Children's prediction errors
6:        $z^t \sim q_{\eta}(z^t \mid \varepsilon_z, z^{t-1})$                                 ▷ Sample coordinate update
7:        $u_z^t \leftarrow \frac{\gamma_{\theta^{t-1}}(z^t; \mathbf{z}_{\setminus z})}{q_{\eta}(z^t \mid \varepsilon_z, z^{t-1})}$                                 ▷ Correct coordinate update by weighing
8:        $z^t \leftarrow \text{RESAMPLE}(z^t, u_z^t)$                                 ▷ Resample from true coordinate update
9:        $\hat{Z}_{\theta^{t-1}}(\mathbf{z}_{\setminus z})^t \leftarrow \frac{1}{K} \sum_{k=1}^K u_z^{t,k}$                                 ▷ Estimate coordinate update's normalizer
10:     $\mathcal{F}^t \leftarrow -\frac{1}{K} \sum_{k=1}^K \log \left( \frac{p_{\theta^{t-1}}(\mathbf{x}, \mathbf{z}^{t,k})}{\prod_{z \in \mathbf{z}} \gamma_{\theta^{t-1}}(z^t; \mathbf{z}_{\setminus z}^{t,k}) \prod_{z \in \mathbf{z}} \hat{Z}_{\theta^{t-1}}(\mathbf{z}_{\setminus z})^t} \right)$                                 ▷ Update free energy
11:     $\theta^t \leftarrow \theta^{t-1} + \eta \frac{1}{K} \sum_{k=1}^K \nabla_{\theta^{t-1}} \log p_{\theta^{t-1}}(\mathbf{x}, \mathbf{z}^{t,k})$                                 ▷ Update parameters
12: return  $\mathbf{z}^T, \theta^T, \mathcal{F}^T$                                 ▷ Output: updated particles, parameters, free energy

```

137 resampling with respect to these weights corrects for discretization error, yields particles distributed
 138 according to the true complete conditional, and estimates the complete conditional's normalizer

$$\text{RESAMPLE}(z^t, u_z^t) \sim \pi_{\theta^{t-1}}(z^t \mid \mathbf{z}_{\setminus z}), \quad \hat{Z}_{\theta^{t-1}}(\mathbf{z}_{\setminus z})^t := \frac{1}{K} \sum_{k=1}^K u_z^{t,k}.$$

139 The recursive step of “Divide and Conquer” Sequential Monte Carlo [Lindsten et al., 2017, Kuntz
 140 et al., 2024] exploits the estimates $\hat{Z}_{\theta^{t-1}}(\mathbf{z}_{\setminus z})^t$ to weigh the samples for the complete target density

$$w_{\theta^{t-1}}^t = \frac{p_{\theta^{t-1}}(\mathbf{x}, \mathbf{z}^t)}{\prod_{z \in \mathbf{z}} \gamma_{\theta^{t-1}}(z^t; \mathbf{z}_{\setminus z}) \prod_{z \in \mathbf{z}} \hat{Z}_{\theta^{t-1}}(\mathbf{z}_{\setminus z})^t}. \quad (8)$$

141 This weight gives rise to a free energy by Proposition 1, whose gradient (Theorem 3 in Appendix B)
 142 equals the expectation, under the proposal, of the complete log-joint density

$$\mathcal{F}^t := \mathbb{E}_q[-\log w_{\theta^{t-1}}^t] \quad \nabla_{\theta^{t-1}} \mathcal{F}^t = \mathbb{E}_q[-\nabla_{\theta^{t-1}} \log p_{\theta^{t-1}}(\mathbf{x}, \mathbf{z}^t)].$$

143 Descending this gradient $\theta^t := \theta^{t-1} - \eta \nabla_{\theta^{t-1}} \mathcal{F}^t$ enables DCPC to learn model parameters θ .

144 The above steps describe a single pass of divide-and-conquer predictive coding over a causal graphical
 145 model. Algorithm 1 shows the complete algorithm, consisting of nested iterations over latent variables
 146 $z \in \mathbf{z}$ (inner loop) and iterations $t \in T$ (outer loop). DCPC satisfies criteria (1) and (2) of Definition 1,
 147 and relaxes criterion (3) to allow gradient-based proposals beyond the Laplace assumption. As with
 148 Pinchetti et al. [2022] and Oliviers et al. [2024], relaxing the Laplace assumption enables much
 149 greater flexibility in approximating the model's true posterior distribution.

150 4 Biological plausibility

151 Different works in the literature consider different criteria for biological plausibility. This paper
 152 follows the non-spiking predictive coding literature and considers an algorithm biologically plausible
 153 if it performs only spatially local computations in a probabilistic graphical model [Whittington and
 154 Bogacz, 2017], without requiring a global control of computation. However, while in the standard
 155 literature locality is either directly defined in the objective function [Rao and Ballard, 1999], or
 156 derived from a mean-field approximation to the joint density [Friston, 2005], showing that the updates
 157 of the parameters of DCPC require only local information is not as trivial. To this end, in this section
 158 we first formally show that DCPC achieves decentralized inference of latent variables \mathbf{z} (Theorem 1),
 159 and then that also the parameters θ are updated via local information (Theorem 2).

160 Gibbs sampling provides the most widely-used algorithm for sampling from a high-dimensional
 161 probability distribution by local signaling. It consists of successively sampling coordinate updates
 162 to individual nodes in the graphical model by targeting their complete conditional densities $\pi_{\theta}(z \mid$
 163 $\mathbf{x}, \mathbf{z}_{\setminus z})$. Theorem 1 demonstrates that DCPC's coordinate updates approximate Gibbs sampling.

164 **Theorem 1** (DCPC coordinate updates sample from the true complete conditionals). *Each DCPC*
 165 *coordinate update (Equation 7) for a latent $z \in \mathbf{z}$ samples from z 's complete conditional (the*
 166 *normalization of Equation 5). Formally, for every measurable $h : \mathcal{Z} \rightarrow \mathbb{R}$, resampled expectations*
 167 *with respect to the DCPC coordinate update equal those with respect to the complete conditional*

$$\mathbb{E}_{z \sim q_\eta(z|z^{t-1}, \epsilon_z^t)} [\mathbb{E}_{u \sim \delta(u), z' \sim \text{RESAMPLE}(z, u_z)} [h(z)]] = \int_{z \in \mathcal{Z}} h(z) \pi_\theta(z | \mathbf{z}_{\setminus z}) dz.$$

168 *Proof.* See Corollary 4.1 in Appendix B. □

169 We follow the canonical cortical microcircuit hypothesis of predictive coding [Bastos et al., 2012,
 170 Gillon et al., 2023] or predictive routing [Bastos et al., 2020]. Consider a cortical column representing
 171 $z \in \mathbf{z}$; the θ , α/β , and γ frequency bands of neuronal oscillations [Buzsáki and Draguhn, 2004]
 172 could synchronize parallelizations (known to exist for simple Gibbs sampling in a causal graphical
 173 model [Gonzalez et al., 2011]) of the loops in Algorithm 1. From the innermost to the outermost and
 174 following the neurophysiological findings of Bastos et al. [2015], Fries [2015], γ -band oscillations
 175 could synchronize the bottom-up conveyance of prediction errors (lines 4-6) from L2/3 of lower
 176 cortical columns to L4 of higher columns, β -band oscillations could synchronize the top-down
 177 conveyance of fresh predictions (implied in passing from s to $s + 1$ in the loop of lines 2-9) from
 178 L5/6 of higher columns to L1+L6 of lower columns, and θ -band oscillations could synchronize
 179 complete attention-directed sampling of stimulus representations (lines 1-11). Figure 5 in Appendix A
 180 visualizes these hypotheses for how neuronal areas and connections could implement DCPC.

181 Biological neurons often spike to represent *changes* in their membrane voltage [Mainen and Sejnowski,
 182 1995, Lundstrom et al., 2008, Forkosh, 2022], and some have even been tested and found to signal
 183 the temporal derivative of the logarithm of an underlying signal [Adler and Alon, 2018, Borba et al.,
 184 2021]. Theorists have also proposed models [Chavlis and Poirazi, 2021, Moldwin et al., 2021]
 185 under which single neurons could calculate gradients internally. In short, if neurons can represent
 186 probability densities, as many theoretical proposals and experiments suggest they can, then they can
 187 likely also calculate the prediction errors used in DCPC. Theorem 2 will demonstrate that given the
 188 “factorization” above, DCPC’s model learning requires only local prediction errors.

189 **Theorem 2** (DCPC parameter learning requires only local gradients in a factorized generative model).
 190 *Consider a graphical model factorized according to Equation 1, with the additional assumption*
 191 *that the model parameters $\theta \in \Theta = \prod_{x \in \mathbf{x}} \Theta_x \times \prod_{z \in \mathbf{z}} \Theta_z$ factorize disjointly. Then the gradient*
 192 *$\nabla_\theta \mathcal{F}(\theta, q)$ of DCPC’s free energy similarly factorizes into a sum of local particle averages*

$$\nabla_\theta \mathcal{F} = \mathbb{E}_q [-\nabla_\theta \log p_\theta(\mathbf{x}, \mathbf{z})] \approx - \sum_{v \in (\mathbf{x}, \mathbf{z})} \frac{1}{K} \sum_{k=1}^K \nabla_{\theta_v} \log p_{\theta_v}(v^k | \text{Pa}(v)^k). \quad (9)$$

193 *Proof.* See Proposition 5 in Appendix B. □

194 Our practical implementation of DCPC, evaluated in the experiments above, takes advantage of
 195 Theorem 2 to save memory by detaching samples from the automatic differentiation graph in the
 196 forward ancestor-sampling pass through the generative model.

197 Finally, DCPC passes from local coordinate updates to the joint target density via an importance
 198 resampling operation, requiring that implementations synchronously transmit numerical densities
 199 or log-densities for the freshly proposed particle population. While phase-locking to a cortical
 200 oscillation may make this biologically feasible, resampling then requires normalizing the weights.
 201 Thankfully, divisive normalization appears ubiquitously throughout the brain [Carandini and Heeger,
 202 2012], as well as just the type of “winner-take-all” circuit that implements a softmax function (e.g. for
 203 normalizing and resampling importance weights) being ubiquitous in crosstalk between superficial
 204 and deep layers of the cortical column [Liu, 1999, Douglas and Martin, 2004].

205 5 Experiments

206 Divide-and-conquer predictive coding is not the first predictive coding algorithm to incorporate
 207 sampling into the inference process, and certainly not the first variational inference algorithm for
 208 structured graphical models. This section therefore evaluates DCPC’s performance against both
 209 models from the predictive coding literature and against a standard deep generative model. Each
 210 experiment holds the generative model, dataset, and hyperparameters constant except where noted.

Inference algorithm	Dataset	NLL ↓	Mean Squared Error ↓
MCPC	MNIST	144.6 ± 0.7	$(8.29 \pm 0.05) \times 10^{-2}$
DCPC	MNIST	102.5 ± 0.01	$0.01 \pm 7.2 \times 10^{-6}$
DCPC	EMNIST	160.8 ± 0.05	$3.3 \times 10^{-6} \pm 3.5 \times 10^{-9}$
DCPC	Fashion MNIST	284.1 ± 0.05	$0.03 \pm 2.7 \times 10^{-5}$

Table 2: Negative log-likelihood and mean squared error for MCPC against DCPC on held-out images from the MNISTs. Means and standard deviations are taken across five random seeds.

We have implemented DCPC as a variational proposal or “guide” program in the deep probabilistic programming language Pyro [Bingham et al., 2019]; doing so enables us to compute free energy and prediction errors efficiently in graphical models involving neural networks. Since the experiments below involve minibatched subsampling of observations $\mathbf{x} \sim \mathcal{B}$ from a dataset $\mathcal{D} \sim p(\mathcal{D})$ of unknown distribution, we replace Equation 9 with a subsampled form (see Welling and Teh [2011] for derivation) of the variational Sequential Monte Carlo gradient estimator [Naesseth et al., 2018]

$$\nabla_{\theta} \mathcal{F} \approx |\mathcal{D}| \mathbb{E}_{\mathcal{B} \sim p(\mathcal{D})} \left[\frac{1}{|\mathcal{B}|} \sum_{\mathbf{x}^b \in \mathcal{B}} \mathbb{E}_{(\mathbf{z}, w)^{1:K} \sim q} \left[\log \left(\frac{1}{K} \sum_{k=1}^K w^k \right) \mid \mathbf{x}^b \right] \right]. \quad (10)$$

We optimized the free energy in all experiments using Adam [Kingma and Ba, 2014], making sure to call `detach()` after every Pyro `sample()` operation to implement the purely local gradient calculations of Theorem 2 and Equation 10. The first experiment below considers a hierarchical Gaussian model on three simple datasets. The model consists of two latent codes above an observation.

Deep latent Gaussian models with predictive coding Oliviers et al. [2024] brought together predictive coding with neural sampling hypotheses in a single model: Monte Carlo predictive coding (MCPC). Their inference algorithm functionally backpropagated the score function of a log-likelihood, applying Langevin proposals to sample latent variables from the posterior joint density along the way. They evaluated MCPC’s performance on MNIST with a deep latent Gaussian model [Rezende et al., 2014] (DLGM). Their model’s conditional densities consisted of nonlinearities followed by linear transformations to parameterize the mean of each Gaussian conditional, with learned covariances. Figure 2 shows that the DLGM structure already requires DCPC to respect hierarchical dependencies.

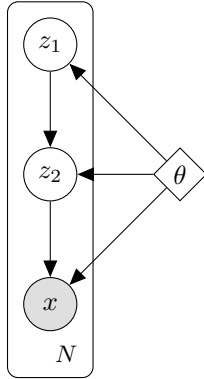


Figure 2: Hierarchical graphical model for DLGM’s.

We tested DCPC’s performance on elementary reconstruction and generation tasks by using it to train this exact generative model, changing only the likelihood from a discrete Bernoulli to a continuous Bernoulli [Loaiza-Ganem and Cunningham, 2019]. After training we evaluated with a discrete Bernoulli likelihood. Table 2 shows that in terms of both surprise (negative log evidence, with the discrete Bernoulli likelihood) and mean squared reconstruction error, DCPC enjoys better average performance with a lower standard deviation of performance, the latter by an order of magnitude. All experiments used a learning rate $\eta = 0.1$ and $K = 4$ particles.

Figure 3 shows an extension of this experiment to EMNIST [Cohen et al., 2017] and Fashion MNIST [Xiao et al., 2017] as well as the original MNIST, with ground-truth images in the top row and their reconstructions from DCPC-inferred latent codes below. The ground-truth images come from a 10% validation split of each data-set, on which DCPC only infers particles $q_{K=4}(\mathbf{z})$.

The above datasets do not typically challenge a new inference algorithm. The next experiment will thus attempt to learn representations of color images, as in the widely-used variational autoencoder [Kingma and Welling, 2013] framework, without an encoder network or amortized inference.

Image generation with representation learning Zahid et al. [2024] have also recently designed and evaluated Langevin predictive coding (LPC), with differences from both MCPC and DCPC. While MCPC sends prediction errors up through a hierarchical model, LPC computed as its prediction error the log-joint gradient for all latent variables in the generative model. This meant that biological plausibility, and their goal of amortizing predictive coding inference, restricted them to single-level decoder adapted from Higgins et al. [2017]. We evaluated with their reported discretized Gaussian likelihood, taken from Cheng et al. [2020], Ho et al. [2020], fixing the variance at $\mathcal{DN}(\mu_{\theta}(\mathbf{z}), 0.01^2)$.

Algorithm	Likelihood	Resolution \uparrow	∇_{θ} -evaluations \times Epochs \downarrow	FID \downarrow
PGD	\mathcal{N}	32×32	1×100	100 ± 2.7
DCPC	\mathcal{N}	32×32	1×100	89.6 ± 0.6
LPC	\mathcal{DN}	64×64	$300 \times 15 = 4500$	120 (approximate)
DCPC	\mathcal{DN}	64×64	$10 \times 450 = 4500$	96.0 ± 0.3

Table 3: FID score comparisons on the CelebA dataset [Liu et al., 2015]. The score for LPC comes from Figure 2 in Zahid et al. [2024], where they ablated warm-starts and initialized from the prior.

We compare DCPC to LPC using the Frechet Inception Distance (FID) [Seitzer, 2020] featured in Zahid et al. [2024], holding constant the prior, neural network architecture, learning rate on θ , and number of gradient evaluations used to train the parameters θ and latents \mathbf{z} . Zahid et al. [2024] evaluated a variety of scenarios and reported that their training could converge quite quickly when counted in epochs, but they accumulated gradients of θ over inference steps. We compare to the results they report after 15 epochs with 300 inference steps applied to latents initialized from the prior, equivalent to $15 \times 300 = 4500$ gradient steps on θ per batch, replicating their batch size of 64. Since Algorithm 1 updates θ only in its outer loop, we set $S = 10$ and ran DCPC for 450 epochs. Table 3 shows that DCPC outperforms LPC in apples-to-apples generative quality, though not to the point of matching state-of-the-art generative model architectures with just a decoder network.

Figure 4 shows reconstructed images from the validation set (left) and samples from the posterior predictive generative model (right). There is blurriness in the reconstructions, as often occurs with variational autoencoders, but DCPC training allows the network to capture background color, hair color, direction in which a face is looking, and other visual properties. Figure 4a shows reconstructions over the validation set, while Figure 4b shows samples from the predictive distribution.

Kuntz et al. [2023] also reported an experiment on CelebA in terms of FID score, at the lower 32×32 resolution. Since they provided both source code and an exact mathematical description, we were able to run an exact, head-to-head comparison with PGD. The line in Table 3 evaluating DCPC with PGD’s example neural architecture at the 32×32 resolution demonstrates a significant improvement in FID for DCPC, alongside a reduction in variance across random samples.

6 Related Work

Pinchetti et al. [2022] expanded predictive coding beyond Gaussian generative models for the first time, applying the resulting algorithm to train variational autoencoders by variational inference and transformer architectures by maximum likelihood. DCPC, in turn, broadens predictive coding to target arbitrary probabilistic graphical models, following the broadening in Salvatori et al. [2022] to arbitrary deterministic computation graphs. DCPC follows on incremental predictive coding [Salvatori et al., 2024] in quickly alternating between updates to random variables and model parameters, giving an incremental EM algorithm [Neal and Hinton, 1998]. Finally, Zahid et al. [2024] and Oliviers et al. [2024] also recognized the analogy between predictive coding’s prediction errors and the score functions used in Langevin dynamics for continuous random variables.

There exists a large body of work on how neurobiologically plausible circuits could implement probabilistic inference. Classic work by Shi and Griffiths [2009] provided a biologically plausible implementation of hierarchical inference via importance sampling; DCPC proceeds from importance sampling as a foundation, while parameterizing the proposal distribution via prediction errors. Recent work by Fang et al. [2022] studied neurally plausible algorithms for sampling-based inference with Langevin dynamics, though only for a Gaussian generative model of sparse coding. Golkar et al. [2022] imposed a whitening constraint on a Gaussian generative model for biological plausibility.

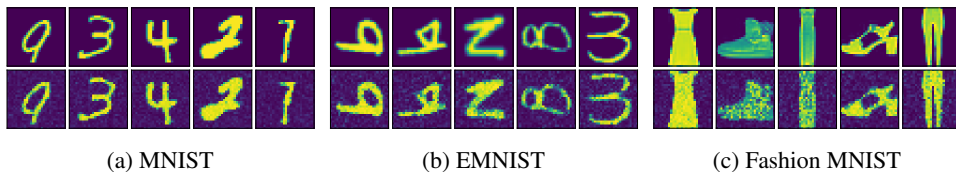
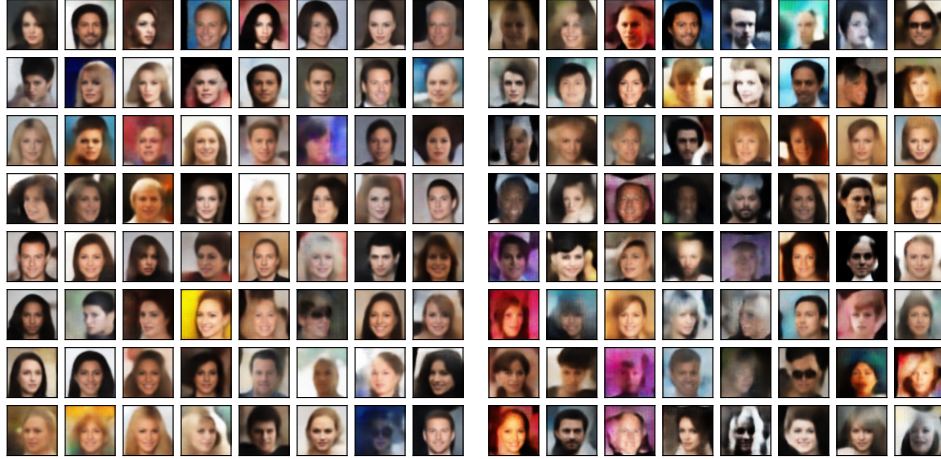


Figure 3: **Top**: images from validation sets of MNIST (left), EMNIST (middle), and Fashion MNIST (right). **Bottom**: reconstructions by deep latent Gaussian models trained with DCPC for MNIST (left), EMNIST (middle), and Fashion MNIST (right), averaging over $K = 4$ particles. DCPC achieves quality reconstructions by inference over \mathbf{z} without training an inference network.



(a) Reconstructions of the CelebA validation set (b) Samples drawn *de novo* from the posterior predictive distribution of the trained network.

Figure 4: **Left:** reconstructions from the CelebA validation set. **Right:** samples from the generative model. DCPC achieves quality reconstructions by inference over \mathbf{z} with $K = 16$ particles and no inference network, while the learned generative model captures variation in the data.

Finally, Dong and Wu [2023] and Zahid et al. [2024] both suggest mechanisms for employing momentum to reduce gradient noise in a biologically plausible sampling algorithm; the former intriguingly analogize their momentum term to neuronal adaptation.

7 Conclusion

This paper proposed divide-and-conquer predictive coding (DCPC), an algorithm that efficiently and scalably approximates Gibbs samplers by importance sampling; DCPC parameterizes efficient proposals for a model’s complete conditional densities using local prediction errors. Section 4 showed how Monte Carlo sampling can implement a form of “prospective configuration” [Song et al., 2024], first inferring a sample from the joint posterior density (Theorem 1) and then updating the generative model without a global backpropagation pass (Theorem 2). Experiments in Section 5 showed that DCPC outperforms the state of the art Monte Carlo Predictive Coding from computational neuroscience, head-to-head, on the simple generative models typically considered in theoretical neuroscience; DCPC also outperforms the particle gradient descent algorithm of Kuntz et al. [2023] while under the constraint of purely local computation. DCPC’s Langevin proposals admit the same extension to constrained sample spaces as applied in Hamiltonian Monte Carlo [Brubaker et al., 2012]; our Pyro implementation includes this extension via Pyro’s preexisting support for HMC.

DCPC offers a number of ways forward. Particularly, this paper employed naive Langevin proposals, while Dong and Wu [2023], Zahid et al. [2024] applied momentum-based preconditioning to take advantage of the target’s geometry. Yin and Ao [2006] demonstrated that gradient flows of this general kind can also provide more efficient samplers by breaking the detailed-balance condition necessary for the Metropolis-Hastings algorithm, motivating the choice of SMC over MCMC to correct proposal bias. Appendix C derives a mathematical background for an extension of DCPC to discrete random variables. Future work could follow Marino et al. [2018], Taniguchi et al. [2022] in using a neural network to iteratively map from particles and prediction errors to proposal parameters.

7.1 Limitations

DCPC’s main limitations are its longer training time, and greater sensitivity to learning rates, than state-of-the-art amortized variational inference trained end-to-end. Such limitations occur frequently in the literature on neuroscience-inspired learning algorithms, as well as in the literature on particle-based algorithms with no parametric form. Scaling up neuroscience-inspired algorithms is an active area of research, and successes in this direction will naturally apply to DCPC, enabling the training of larger models on more complex datasets by predictive coding. This work has no singular ethical concerns specific only to DCPC, rather than the broader implications and responsibilities accompanying advancements in biologically plausible learning and Bayesian inference.

References

- Miri Adler and Uri Alon. Fold-change detection in biological systems. *Current Opinion in Systems Biology*, 8:81–89, April 2018. ISSN 2452-3100. doi: 10.1016/j.coisb.2017.12.005.
- Lisa Feldman Barrett. Context reconsidered: Complex signal ensembles, relational meaning, and population thinking in psychological science. *American Psychologist*, 77(8):894, 2022.
- Andre M Bastos, Julien Vezoli, and Pascal Fries. Communication through coherence with inter-areal delays. *Current Opinion in Neurobiology*, 31:173–180, April 2015. ISSN 09594388. doi: 10.1016/j.conb.2014.11.001.
- André M. Bastos, W Martin Usrey, Rick A Adams, George R Mangun, Pascal Fries, and Karl J Friston. Canonical microcircuits for predictive coding. *Neuron*, 76(4):695–711, 2012.
- André M. Bastos, Mikael Lundqvist, Ayan S. Waite, Nancy Kopell, and Earl K. Miller. Layer and rhythm specificity for predictive routing. *Proceedings of the National Academy of Sciences*, 117(49):31459–31469, December 2020. ISSN 0027-8424, 1091-6490. doi: 10.1073/pnas.2014868117.
- Johanna Bergmann, Lucy S Petro, Clement Abbatecola, Min S Li, A Tyler Morgan, and Lars Muckli. Cortical depth profiles in primary visual cortex for illusory and imaginary experiences. *Nature Communications*, 15(1):1002, 2024.
- Eli Bingham, Jonathan P. Chen, Martin Jankowiak, Fritz Obermeyer, Neeraj Pradhan, Theofanis Karaletsos, Rohit Singh, Paul Szerlip, Paul Horsfall, and Noah D. Goodman. Pyro: Deep universal probabilistic programming. *Journal of Machine Learning Research*, 20(28):1–6, 2019. URL <http://jmlr.org/papers/v20/18-403.html>.
- Cezar Borba, Matthew J Kourakis, Shea Schwennicke, Lorena Brasnic, and William C Smith. Fold change detection in visual processing. *Frontiers in Neural Circuits*, 15:705161, 2021.
- Marcus Brubaker, Mathieu Salzmann, and Raquel Urtasun. A family of mcmc methods on implicitly defined manifolds. In *Artificial intelligence and statistics*, pages 161–172. PMLR, 2012.
- György Buzsáki and Andreas Draguhn. Neuronal oscillations in cortical networks. *Science*, 304(5679):1926–1929, June 2004. ISSN 0036-8075, 1095-9203. doi: 10.1126/science.1099745.
- Luke Campagnola, Stephanie C. Seeman, Thomas Chartrand, Lisa Kim, Alex Hoggarth, Clare Gamlin, Shinya Ito, Jessica Trinh, Pasha Davoudian, Cristina Radaelli, Mean-Hwan Kim, Travis Hage, Thomas Braun, Lauren Alfiler, Julia Andrade, Phillip Bohn, Rachel Dalley, Alex Henry, Sara Kebede, Alice Mukora, David Sandman, Grace Williams, Rachael Larsen, Corinne Teeter, Tanya L. Daigle, Kyla Berry, Nadia Dotson, Rachel Enstrom, Melissa Gorham, Madie Hupp, Samuel Dingman Lee, Kiet Ngo, Philip R. Nicovich, Lydia Potekhina, Shea Ransford, Amanda Gary, Jeff Goldy, Delissa McMillen, Trangthanh Pham, Michael Tieu, La’Akea Siverts, Miranda Walker, Colin Farrell, Martin Schroedter, Cliff Slaughterbeck, Charles Cobb, Richard Ellenbogen, Ryder P. Gwinn, C. Dirk Keene, Andrew L. Ko, Jeffrey G. Ojemann, Daniel L. Silbergeld, Daniel Carey, Tamara Casper, Kirsten Crichton, Michael Clark, Nick Dee, Lauren Ellingwood, Jessica Gloe, Matthew Kroll, Josef Sulc, Herman Tung, Katherine Wadhwani, Krissy Brouner, Tom Egdorf, Michelle Maxwell, Medea McGraw, Christina Alice Pom, Augustin Ruiz, Jasmine Bomben, David Feng, Nika Hejazinia, Shu Shi, Aaron Szafer, Wayne Wakeman, John Phillips, Amy Bernard, Luke Eposito, Florence D. D’Orazi, Susan Sunkin, Kimberly Smith, Bosiljka Tasic, Anton Arkhipov, Staci Sorensen, Ed Lein, Christof Koch, Gabe Murphy, Hongkui Zeng, and Tim Jarsky. Local connectivity and synaptic dynamics in mouse and human neocortex. *Science*, 375(6585):eabj5861, 2022. doi: 10.1126/science.abj5861. URL <https://www.science.org/doi/abs/10.1126/science.abj5861>.
- Matteo Carandini and David J Heeger. Normalization as a canonical neural computation. *Nature reviews neuroscience*, 13(1):51–62, 2012.
- Nick Chater, Joshua B Tenenbaum, and Alan Yuille. Probabilistic models of cognition: Conceptual foundations. *Trends in cognitive sciences*, 10(7):287–291, 2006.

372 Spyridon Chavlis and Panayiota Poirazi. Drawing inspiration from biological dendrites to empower
373 artificial neural networks. *Current Opinion in Neurobiology*, 70:1–10, October 2021. ISSN
374 0959-4388. doi: 10.1016/j.conb.2021.04.007.

375 Zhengxue Cheng, Heming Sun, Masaru Takeuchi, and Jiro Katto. Learned image compression
376 with discretized gaussian mixture likelihoods and attention modules. In *Proceedings of the 2020*
377 *IEEE/CVF Conference on Computer Vision and Pattern Recognition (CVPR)*, 2020.

378 Gregory Cohen, Saeed Afshar, Jonathan Tapson, and Andre Van Schaik. Emnist: Extending mnist to
379 handwritten letters. In *2017 international joint conference on neural networks (IJCNN)*, pages
380 2921–2926. IEEE, 2017.

381 Ishita Dasgupta, Eric Schulz, Joshua B Tenenbaum, and Samuel J Gershman. A theory of learning to
382 infer. *Psychological review*, 127(3):412, 2020.

383 Xingsi Dong and Si Wu. Neural Sampling in Hierarchical Exponential-family Energy-based Models.
384 In *Advances in Neural Information Processing Systems*, New Orleans, LA, 2023. Curran Associates
385 Inc.

386 Rodney J Douglas and Kevan AC Martin. Neuronal circuits of the neocortex. *Annu. Rev. Neurosci.*,
387 27(1):419–451, 2004.

388 Kenji Doya. *Bayesian brain: Probabilistic approaches to neural coding*. MIT press, 2007.

389 Michael Y-S Fang, Mayur Mudigonda, Ryan Zarccone, Amir Khosrowshahi, and Bruno A Olshausen.
390 Learning and inference in sparse coding models with langevin dynamics. *Neural Computation*, 34
391 (8):1676–1700, 2022.

392 Oren Forkosh. Memoryless optimality: Neurons do not need adaptation to optimally encode stimuli
393 with arbitrarily complex statistics. *Neural Computation*, 34(12):2374–2387, November 2022.
394 ISSN 0899-7667, 1530-888X. doi: 10.1162/neco_a_01543.

395 Pascal Fries. Rhythms for cognition: Communication through coherence. *Neuron*, 88(1):220–235,
396 October 2015. ISSN 0896-6273. doi: 10.1016/j.neuron.2015.09.034.

397 Karl Friston. A theory of cortical responses. *Philosophical transactions of the Royal Society B:*
398 *Biological sciences*, 360(1456):815–836, 2005.

399 Karl Friston, James Kilner, and Lee Harrison. A free energy principle for the brain. *Journal*
400 *of Physiology-Paris*, 100(1):70–87, 2006. ISSN 0928-4257. doi: [https://doi.org/10.1016/j.](https://doi.org/10.1016/j.jphysparis.2006.10.001)
401 [jphysparis.2006.10.001](https://doi.org/10.1016/j.jphysparis.2006.10.001). URL [https://www.sciencedirect.com/science/article/pii/](https://www.sciencedirect.com/science/article/pii/S092842570600060X)
402 [S092842570600060X](https://www.sciencedirect.com/science/article/pii/S092842570600060X). Theoretical and Computational Neuroscience: Understanding Brain Func-
403 tions.

404 Colleen J. Gillon, Jason E. Pina, Jérôme A. Lecoq, Ruweida Ahmed, Yazan N. Billeh, Shiella
405 Caldejon, Peter Groblewski, Timothy M. Henley, India Kato, Eric Lee, Jennifer Luviano, Kyla
406 Mace, Chelsea Nayan, Thuyanh V. Nguyen, Kat North, Jed Perkins, Sam Seid, Matthew T. Valley,
407 Ali Williford, Yoshua Bengio, Timothy P. Lillicrap, Blake A. Richards, and Joel Zylberberg.
408 Learning from unexpected events in the neocortical microcircuit. *bioRxiv*, 2023. doi: 10.1101/
409 2021.01.15.426915. URL [https://www.biorxiv.org/content/early/2023/04/06/2021.](https://www.biorxiv.org/content/early/2023/04/06/2021.01.15.426915)
410 [01.15.426915](https://www.biorxiv.org/content/early/2023/04/06/2021.01.15.426915).

411 Siavash Golkar, Tiberiu Tesileanu, Yanis Bahroun, Anirvan Sengupta, and Dmitri Chklovskii.
412 Constrained predictive coding as a biologically plausible model of the cortical hierarchy. In
413 S. Koyejo, S. Mohamed, A. Agarwal, D. Belgrave, K. Cho, and A. Oh, editors, *Advances in*
414 *Neural Information Processing Systems*, volume 35, pages 14155–14169. Curran Associates,
415 Inc., 2022. URL [https://proceedings.neurips.cc/paper_files/paper/2022/file/](https://proceedings.neurips.cc/paper_files/paper/2022/file/5b5de8526aac159e37ff9547713677ed-Paper-Conference.pdf)
416 [5b5de8526aac159e37ff9547713677ed-Paper-Conference.pdf](https://proceedings.neurips.cc/paper_files/paper/2022/file/5b5de8526aac159e37ff9547713677ed-Paper-Conference.pdf).

417 Joseph Gonzalez, Yucheng Low, Arthur Gretton, and Carlos Guestrin. Parallel gibbs sampling:
418 From colored fields to thin junction trees. In Geoffrey Gordon, David Dunson, and Miroslav
419 Dudík, editors, *Proceedings of the Fourteenth International Conference on Artificial Intelligence*
420 *and Statistics*, volume 15 of *Proceedings of Machine Learning Research*, pages 324–332, Fort
421 Lauderdale, FL, USA, 11–13 Apr 2011. PMLR. URL [https://proceedings.mlr.press/](https://proceedings.mlr.press/v15/gonzalez11a.html)
422 [v15/gonzalez11a.html](https://proceedings.mlr.press/v15/gonzalez11a.html).

423 Irina Higgins, Loic Matthey, Arka Pal, Christopher Burgess, Xavier Glorot, Matthew Botvinick,
424 Shakir Mohamed, and Alexander Lerchner. beta-VAE: Learning basic visual concepts with a
425 constrained variational framework. In *International Conference on Learning Representations*,
426 2017. URL <https://openreview.net/forum?id=Sy2fzU9gl>.

427 Jonathan Ho, Ajay Jain, and Pieter Abbeel. Denoising diffusion probabilistic models. In
428 *Advances in Neural Information Processing Systems*, volume 33, page 6840–6851. Cur-
429 ran Associates, Inc., 2020. URL [https://proceedings.neurips.cc/paper/2020/hash/](https://proceedings.neurips.cc/paper/2020/hash/4c5bcfec8584af0d967f1ab10179ca4b-Abstract.html)
430 [4c5bcfec8584af0d967f1ab10179ca4b-Abstract.html](https://proceedings.neurips.cc/paper/2020/hash/4c5bcfec8584af0d967f1ab10179ca4b-Abstract.html).

431 Katie Hoemann, Maria Gendron, and Lisa Feldman Barrett. Mixed emotions in the predictive
432 brain. *Current Opinion in Behavioral Sciences*, 15:51–57, 2017. ISSN 2352-1546. doi: <https://doi.org/10.1016/j.cobeha.2017.05.013>. URL [https://www.sciencedirect.com/science/](https://www.sciencedirect.com/science/article/pii/S2352154616302686)
433 [article/pii/S2352154616302686](https://www.sciencedirect.com/science/article/pii/S2352154616302686). Mixed emotions.
434

435 J. Benjamin Hutchinson and Lisa Feldman Barrett. The Power of Predictions: An Emerging Paradigm
436 for Psychological Research. *Current Directions in Psychological Science*, 2019. ISSN 14678721.
437 doi: 10.1177/0963721419831992.

438 Diederik P Kingma and Jimmy Ba. Adam: A method for stochastic optimization. *arXiv preprint*
439 *arXiv:1412.6980*, 2014.

440 Diederik P Kingma and Max Welling. Auto-encoding variational bayes. *arXiv preprint*
441 *arXiv:1312.6114*, 2013.

442 Juan Kuntz, Jen Ning Lim, and Adam M Johansen. Particle algorithms for maximum likelihood
443 training of latent variable models. In *Proceedings of the 26th International Conference on Artificial*
444 *Intelligence and Statistics*, volume 206, Valencia, Spain, April 2023. Proceedings of Machine
445 Learning Research.

446 Juan Kuntz, Francesca R. Crucinio, and Adam M. Johansen. The divide-and-conquer sequential Monte
447 Carlo algorithm: Theoretical properties and limit theorems. *The Annals of Applied Probability*,
448 34(1B):1469 – 1523, 2024. doi: 10.1214/23-AAP1996. URL [https://doi.org/10.1214/](https://doi.org/10.1214/23-AAP1996)
449 [23-AAP1996](https://doi.org/10.1214/23-AAP1996).

450 Brenden M. Lake, Tomer D. Ullman, Joshua B. Tenenbaum, and Samuel J. Gershman. Building
451 machines that learn and think like people. *Behavioral and Brain Sciences*, 40:e253, 2017. doi:
452 10.1017/S0140525X16001837.

453 Yann Lecun, Yoshua Bengio, and Geoffrey Hinton. Deep learning. *Nature*, 521(7553):436–444,
454 2015. ISSN 14764687. doi: 10.1038/nature14539. Citation Key: Lecun2015.

455 F. Lindsten, A. M. Johansen, C. A. Naesseth, B. Kirkpatrick, T. B. Schön, J. A.D. Aston, and
456 A. Bouchard-Côté. Divide-and-conquer with sequential monte carlo. *Journal of Computational and*
457 *Graphical Statistics*, 26(2):445–458, 2017. ISSN 15372715. doi: 10.1080/10618600.2016.1237363.
458 arXiv: 1406.4993 Citation Key: Lindsten2017.

459 Shih-Chii Liu. A winner-take-all circuit with controllable soft max property. In S. Solla, T. Leen,
460 and K. Müller, editors, *Advances in Neural Information Processing Systems*, volume 12. MIT
461 Press, 1999. URL [https://proceedings.neurips.cc/paper_files/paper/1999/file/](https://proceedings.neurips.cc/paper_files/paper/1999/file/3e7e0224018ab3cf51abb96464d518cd-Paper.pdf)
462 [3e7e0224018ab3cf51abb96464d518cd-Paper.pdf](https://proceedings.neurips.cc/paper_files/paper/1999/file/3e7e0224018ab3cf51abb96464d518cd-Paper.pdf).

463 Ziwei Liu, Ping Luo, Xiaogang Wang, and Xiaoou Tang. Deep learning face attributes in the wild. In
464 *Proceedings of International Conference on Computer Vision (ICCV)*, December 2015.

465 Gabriel Loaiza-Ganem and John P Cunningham. The continuous bernoulli: fixing a pervasive error
466 in variational autoencoders. In *Advances in Neural Information Processing Systems*, volume 32.
467 Curran Associates, Inc., 2019. URL [https://proceedings.neurips.cc/paper/2019/hash/](https://proceedings.neurips.cc/paper/2019/hash/f82798ec8909d23e55679ee26bb26437-Abstract.html)
468 [f82798ec8909d23e55679ee26bb26437-Abstract.html](https://proceedings.neurips.cc/paper/2019/hash/f82798ec8909d23e55679ee26bb26437-Abstract.html).

469 Brian N. Lundstrom, Matthew H. Higgs, William J. Spain, and Adrienne L. Fairhall. Fractional differ-
470 entiation by neocortical pyramidal neurons. *Nature Neuroscience*, 11(11):1335–1342, November
471 2008. ISSN 1546-1726. doi: 10.1038/nn.2212.

472 Zachary F Mainen and Terrence J Sejnowski. Reliability of spike timing in neocortical neurons.
473 *Science*, 268(5216):1503–1506, 1995.

474 Joseph Marino, Yisong Yue, and Stephan Mandt. Iterative amortized inference. In *35th International*
475 *Conference on Machine Learning, ICML 2018*, volume 8, page 5444–5462, 2018. ISBN 978-1-
476 5108-6796-3. arXiv: 1807.09356 Citation Key: Marino2018a.

477 Beren Millidge, Anil Seth, and Christopher L Buckley. Predictive coding: a theoretical and experi-
478 mental review. *arXiv preprint arXiv:2107.12979*, 2021.

479 Beren Millidge, Yuhang Song, Tommaso Salvatori, Thomas Lukasiewicz, and Rafal Bogacz. A
480 theoretical framework for inference and learning in predictive coding networks. In *The Eleventh*
481 *International Conference on Learning Representations*, 2023. URL [https://openreview.net/](https://openreview.net/forum?id=ZCTvSF_uVM4)
482 [forum?id=ZCTvSF_uVM4](https://openreview.net/forum?id=ZCTvSF_uVM4).

483 Toviah Moldwin, Menachem Kalmenson, and Idan Segev. The gradient clusteron: A model neuron
484 that learns to solve classification tasks via dendritic nonlinearities, structural plasticity, and gradient
485 descent. *PLOS Computational Biology*, 17(5):e1009015, May 2021. ISSN 1553-7358. doi:
486 10.1371/journal.pcbi.1009015.

487 Christian Naesseth, Fredrik Lindsten, and Thomas Schon. Nested sequential monte carlo methods.
488 In Francis Bach and David Blei, editors, *Proceedings of the 32nd International Conference*
489 *on Machine Learning*, volume 37 of *Proceedings of Machine Learning Research*, pages 1292–
490 1301, Lille, France, 07–09 Jul 2015. PMLR. URL [https://proceedings.mlr.press/v37/](https://proceedings.mlr.press/v37/naesseth15.html)
491 [naesseth15.html](https://proceedings.mlr.press/v37/naesseth15.html).

492 Christian Naesseth, Scott Linderman, Rajesh Ranganath, and David Blei. Variational sequen-
493 tial monte carlo. In Amos Storkey and Fernando Perez-Cruz, editors, *Proceedings of the*
494 *Twenty-First International Conference on Artificial Intelligence and Statistics*, volume 84 of
495 *Proceedings of Machine Learning Research*, pages 968–977. PMLR, 09–11 Apr 2018. URL
496 <https://proceedings.mlr.press/v84/naesseth18a.html>.

497 Radford M. Neal and Geoffrey E. Hinton. *A View of the EM Algorithm that Justifies Incremental,*
498 *Sparse, and other Variants*, page 355–368. NATO ASI Series. Springer Netherlands, Dordrecht,
499 1998, ISBN 978-94-011-5014-9. doi: 10.1007/978-94-011-5014-9_12. URL [https://doi.org/](https://doi.org/10.1007/978-94-011-5014-9_12)
500 [10.1007/978-94-011-5014-9_12](https://doi.org/10.1007/978-94-011-5014-9_12).

501 Gaspard Oliviers, Rafal Bogacz, and Alexander Meulemans. Learning probability distributions of
502 sensory inputs with monte carlo predictive coding. *bioRxiv*, 2024.

503 Benjamin Peters, James J DiCarlo, Todd Gureckis, Ralf Haefner, Leyla Isik, Joshua Tenenbaum, Talia
504 Konkle, Thomas Naselaris, Kimberly Stachenfeld, Zenna Tavares, et al. How does the primate
505 brain combine generative and discriminative computations in vision? *ArXiv*, 2024.

506 Luca Pinchetti, Tommaso Salvatori, Yordan Yordanov, Beren Millidge, Yuhang Song, and
507 Thomas Lukasiewicz. Predictive coding beyond gaussian distributions. In S. Koyejo,
508 S. Mohamed, A. Agarwal, D. Belgrave, K. Cho, and A. Oh, editors, *Advances in Neu-*
509 *ral Information Processing Systems*, volume 35, pages 1280–1293. Curran Associates,
510 Inc., 2022. URL [https://proceedings.neurips.cc/paper_files/paper/2022/file/](https://proceedings.neurips.cc/paper_files/paper/2022/file/08f9de0232c0b485110237f6e6cf88f1-Paper-Conference.pdf)
511 [08f9de0232c0b485110237f6e6cf88f1-Paper-Conference.pdf](https://proceedings.neurips.cc/paper_files/paper/2022/file/08f9de0232c0b485110237f6e6cf88f1-Paper-Conference.pdf).

512 Alexandre Pouget, Jeffrey M Beck, Wei Ji Ma, and Peter E Latham. Probabilistic brains: knowns and
513 unknowns. *Nature neuroscience*, 16(9):1170–1178, 2013.

514 Rajesh P N Rao and Dana H Ballard. Predictive coding in the visual cortex: a functional interpretation
515 of some extra-classical receptive-field effects. *Nature neuroscience*, 2(1):79–87, 1999. ISSN
516 1097-6256. doi: 10.1038/4580. URL 10.1038/4580%5Cnhttp://www.nature.com/neuro/
517 [journal/v2/n1/abs/nn0199_79.html](http://www.nature.com/neuro/journal/v2/n1/abs/nn0199_79.html).

518 Danilo Jimenez Rezende, Shakir Mohamed, and Daan Wierstra. Stochastic backpropagation and
519 approximate inference in deep generative models. In *Proceedings of the 31st International*
520 *Conference on Machine Learning*, volume 4, page 3057–3070, Beijing, China, 2014. arXiv:
521 1401.4082 Citation Key: Rezende2014 ISBN: 9781634393973.

David E Rumelhart, Geoffrey E Hinton, and Ronald J Williams. Learning representations by back-propagating errors. *Nature*, 323(6088):533–536, 1986.

Tommaso Salvatori, Luca Pinchetti, Beren Millidge, Yuhang Song, Tianyi Bao, Rafal Bogacz, and Thomas Lukasiewicz. Learning on arbitrary graph topologies via predictive coding. *Advances in neural information processing systems*, 35:38232–38244, 2022.

Tommaso Salvatori, Ankur Mali, Christopher L Buckley, Thomas Lukasiewicz, Rajesh PN Rao, Karl Friston, and Alexander Ororbia. Brain-inspired computational intelligence via predictive coding. *arXiv preprint arXiv:2308.07870*, 2023.

Tommaso Salvatori, Yuhang Song, Yordan Yordanov, Beren Millidge, Cornelius Emde, Zhenghua Xu, Lei Sha, Rafal Bogacz, and Thomas Lukasiewicz. A stable, fast, and fully automatic learning algorithm for predictive coding networks. In *International Conference on Learning Representations*, 2024.

Jürgen Schmidhuber. Deep learning in neural networks: An overview. *Neural Networks*, 61:85–117, 2015. ISSN 18792782. doi: 10.1016/j.neunet.2014.09.003. Citation Key: Schmidhuber2015.

Maximilian Seitzer. pytorch-fid: FID Score for PyTorch. <https://github.com/mseitzer/pytorch-fid>, August 2020. Version 0.3.0.

Lei Shi and Thomas L. Griffiths. Neural implementation of hierarchical bayesian inference by importance sampling. In *Advances in Neural Information Processing Systems*, page 1669–1677, 2009. ISBN 978-1-61567-911-9. Citation Key: Shi2009.

Yuhang Song, Beren Millidge, Tommaso Salvatori, Thomas Lukasiewicz, Zhenghua Xu, and Rafal Bogacz. Inferring neural activity before plasticity as a foundation for learning beyond backpropagation. *Nature Neuroscience*, page 1–11, January 2024. ISSN 1546-1726. doi: 10.1038/s41593-023-01514-1.

M. W. Spratling. A review of predictive coding algorithms. *Brain and Cognition*, 112:92–97, 2017. ISSN 10902147. doi: 10.1016/j.bandc.2015.11.003.

M. V. Srinivasan, S. B. Laughlin, and A. Dubs. Predictive coding: A fresh view of inhibition in the retina. *Proceedings of the Royal Society of London - Biological Sciences*, 216(1205):427–459, 1982. ISSN 09628452. doi: 10.1098/rspb.1982.0085.

Sam Stites, Heiko Zimmermann, Hao Wu, Eli Sennesh, and Jan-Willem Van de Meent. Learning proposals for probabilistic programs with inference combinators. *37th Conference on Uncertainty in Artificial Intelligence (UAI 2021)*, 2021.

Shohei Taniguchi, Yusuke Iwasawa, Wataru Kumagai, and Yutaka Matsuo. Langevin autoencoders for learning deep latent variable models. *Advances in Neural Information Processing Systems*, 35: 13277–13289, 2022. URL https://proceedings.neurips.cc/paper_files/paper/2022/hash/565f995643da6329cec701f26f8579f5-Abstract-Conference.html.

Stefan Webb, Adam Golinski, Rob Zinkov, Siddharth N, Tom Rainforth, Yee Whye Teh, and Frank Wood. Faithful inversion of generative models for effective amortized inference. In S. Bengio, H. Wallach, H. Larochelle, K. Grauman, N. Cesa-Bianchi, and R. Garnett, editors, *Advances in Neural Information Processing Systems*, volume 31. Curran Associates, Inc., 2018. URL https://proceedings.neurips.cc/paper_files/paper/2018/file/894b77f805bd94d292574c38c5d628d5-Paper.pdf.

Max Welling and Yee Whye Teh. Bayesian learning via stochastic gradient langevin dynamics. In *Proceedings of the 28th International Conference on Machine Learning, ICML 2011*, Bellevue, WA, USA, 2011. Proceedings of Machine Learning Research.

James CR Whittington and Rafal Bogacz. An approximation of the error backpropagation algorithm in a predictive coding network with local hebbian synaptic plasticity. *Neural computation*, 29(5): 1229–1262, 2017.

Han Xiao, Kashif Rasul, and Roland Vollgraf. Fashion-mnist: a novel image dataset for benchmarking machine learning algorithms. *arXiv preprint arXiv:1708.07747*, 2017.

- 571 L. Yin and P. Ao. Existence and construction of dynamical potential in nonequilibrium processes
572 without detailed balance. *Journal of Physics A: Mathematical and General*, 39(27):8593, June
573 2006. ISSN 0305-4470. doi: 10.1088/0305-4470/39/27/003. URL [https://dx.doi.org/10.](https://dx.doi.org/10.1088/0305-4470/39/27/003)
574 1088/0305-4470/39/27/003.
- 575 Umais Zahid, Qinghai Guo, and Zafeirios Fountas. Sample as you infer: Predictive coding with
576 langevin dynamics. In *Proceedings of the 41st International Conference on Machine Learning*,
577 volume 235, Vienna, Austria, 2024. Proceedings of Machine Learning Research.

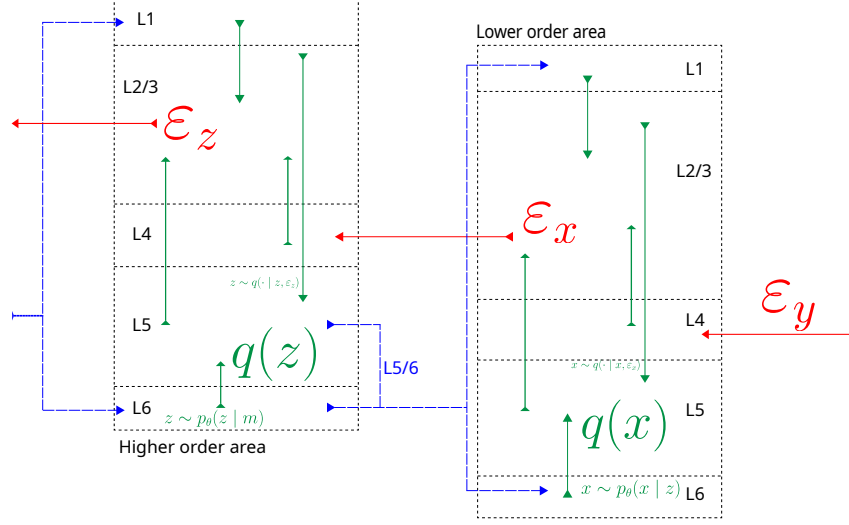


Figure 5: Divide-and-conquer predictive coding provides an algorithmic interpretation for some of the connections mapped in the canonical neocortical microcircuit [Bastos et al., 2012, 2020, Campagnola et al., 2022]: prediction errors (red) arrive through ascending pathways into the central laminar layer 4, which transmits them up to layers 2/3 (green). These layers combine the incoming errors with a present posterior estimate (green L5→L2/3 connection) to generate prediction errors for the next cortical area. Eventually the updated predictions flow back down the cortical hierarchy (blue).

578 A Further experiments and results

579 **Alternate image generation/ representation learning** As indicated in Section 2, this paper builds
 580 upon the particle gradient descent (PGD) algorithm; Kuntz et al. [2023] demonstrated the algorithm’s
 581 performance by training a generator network on CelebA. Their network employed a Gaussian
 582 likelihood with a fixed standard deviation of 0.01, and evaluated a log-joint objective over 100 epochs
 583 on exactly 10,000 subsampled data points. The paper then evaluated mean squared error on an
 584 inpainting task and the Frechet Inception Distance over data images.

585 When applied to the resulting target density, DCPC amounts to PGD with a resampling step. Table 4
 586 shows the results of training and evaluating the same model described above with DCPC. Since PGD
 587 trained for 100 epochs with a batch size of 128, albeit on a 10,000-image subsample of CelebA, we
 588 trained with the entire dataset for 100 epochs with batch-size 128.

Inference type	Log-joint	FID ↓
PGD ($K = 10$)	-3.8×10^5	100 ± 2.7
DCPC (ours, $K = 10$)	-3.0×10^6	89.6 ± 0.6

Table 4: Log-joint probabilities and FID metrics show how DCPC performs against the original PGD.

589 We suspect that the supplied code for log-joint calculation averages over either particles or batch items
 590 differently from how we have evaluated DCPC (e.g. we call `mean()` without dividing by any further
 591 shape dimensions), accounting for the apparent order-of-magnitude difference between log-joints.

592 At the request of reviewers, we have substituted a simplified Figure 1 in the main text for Figure 5
 593 showing how to map DCPC onto laminar microcircuit structure.

594 B Importance sampling and gradient estimation proofs

595 **Definition 2** (Strict proper weighting for a density). *Given an unnormalized density $\gamma_\theta(\mathbf{z})$ with*
 596 *corresponding normalizing constant $Z(\theta)$ and normalized density $\pi_\theta(\mathbf{z})$*

$$Z(\theta) := \int_{\mathbf{z} \in \mathcal{Z}} \gamma_\theta(\mathbf{z}) d\mathbf{z} \quad \pi_\theta(\mathbf{z}) := \frac{\gamma_\theta(\mathbf{z})}{Z(\theta)},$$

597 the random variables $w, \mathbf{z} \sim q(w, \mathbf{z})$ are strictly properly weighted [Naesseth et al., 2015] with
 598 respect to $\gamma_\theta(\mathbf{z})$ if and only if for any measurable test function $h : \mathcal{Z} \rightarrow \mathbb{R}$, the weighted expectation
 599 over the proposal $q(w, \mathbf{z})$ equals the expectation under the target $\gamma_\theta(\mathbf{z})$

$$\mathbb{E}_{w, \mathbf{z} \sim q(w, \mathbf{z})} [wh(\mathbf{z})] = \int_{\mathbf{z} \in \mathcal{Z}} h(\mathbf{z}) \gamma_\theta(\mathbf{z}) d\mathbf{z}. \quad (11)$$

600 The first two propositions come from the previous work by Wu et al. [2020], Stites et al. [2021] and
 601 Zimmermann et al. [2021]. The reader looking for foundations can see Naesseth et al. [2015] or
 602 Chopin and Papaspiliopoulos [2020].

603 **Proposition 1** (The free energy upper-bounds the surprisal). *Given a proposal $q_\phi(w, \mathbf{z})$ strictly*
 604 *properly weighted (Definition 2) for the target $\gamma_\theta(\mathbf{z})$, the variational free energy provides an upper*
 605 *bound to the target’s surprisal*

$$\mathcal{F}(\theta, q) \geq -\log Z(\theta). \quad (12)$$

606 *Proof.* I begin by writing out the free energy (Equation 2) as an expectation of a negative logarithm

$$\mathcal{F}(\theta, q) = \mathbb{E}_{z, w \sim q(z, w)} [-\log w].$$

607 Jensen’s Inequality allows moving the expectation into the negative logarithm by relaxing the
 608 definition of the variational free energy from an equality to an upper bound

$$\mathcal{F}(\theta, q) \geq -\log \mathbb{E}_{z, w \sim q(z, w)} [w].$$

609 Setting $h(z) = 1$, strict proper weighting for an unnormalized density (Definition 2) says the expected
 610 weight will be the normalizing constant

$$\mathbb{E}_{z, w \sim q(z, w)} [w] = Z(\theta)$$

611 which I substitute back in to obtain the desired inequality $\mathcal{F}(\theta, q) \geq -\log Z(\theta)$. \square

612 **Proposition 2** (Weighted expectations approximate the normalized target up to a constant). *Given*
 613 *a proposal $q_\phi(w, \mathbf{z})$ strictly properly weighted (Definition 2) for the target $\gamma_\theta(\mathbf{z})$ and a measurable*
 614 *test function $h : \mathcal{Z} \rightarrow \mathbb{R}$, weighted expectations under the proposal equal the target’s normalizing*
 615 *constant times the test function’s expectation under the normalized target*

$$\mathbb{E}_{(w, \mathbf{z}) \sim q_\phi(w, \mathbf{z})} [wh(\mathbf{z})] = Z(\theta) \mathbb{E}_{\mathbf{z} \sim \pi_\theta(\cdot)} [h(\mathbf{z})].$$

616 *Proof.* Strict proper weighting (Equation 11) states that weighted expectations under the proposal
 617 equal integrals over the unnormalized target, and by definition the normalized target equals the
 618 unnormalized density over its normalizing constant

$$\mathbb{E}_{w, \mathbf{z} \sim q(w, \mathbf{z})} [wh(\mathbf{z})] = \int_{\mathbf{z} \in \mathcal{Z}} h(\mathbf{z}) \gamma_\theta(\mathbf{z}) d\mathbf{z}, \quad \pi_\theta(\mathbf{z}) := \frac{\gamma_\theta(\mathbf{z})}{Z(\theta)}.$$

619 The second equation expresses the unnormalized target in terms of the normalized one

$$Z(\theta) \pi_\theta(\mathbf{z}) = \gamma_\theta(\mathbf{z}),$$

620 and substituting this expression into the definition of strict proper weighting leads to the desired result

$$\begin{aligned} \int_{\mathbf{z} \in \mathcal{Z}} h(\mathbf{z}) \gamma_\theta(\mathbf{z}) d\mathbf{z} &= \int_{\mathbf{z} \in \mathcal{Z}} h(\mathbf{z}) Z(\theta) \pi_\theta(\mathbf{z}) d\mathbf{z}, \\ &= Z(\theta) \int_{\mathbf{z} \in \mathcal{Z}} h(\mathbf{z}) \pi_\theta(\mathbf{z}) d\mathbf{z} \\ \mathbb{E}_{w, \mathbf{z} \sim q(w, \mathbf{z})} [wh(\mathbf{z})] &= Z(\theta) \mathbb{E}_{\pi_\theta(\mathbf{z})} [h(\mathbf{z})]. \end{aligned} \quad \square$$

621 **Proposition 3** (DCPC’s free energy has a pathwise derivative). *The free energy $\mathcal{F}^{t+1} =$*
 622 *$\mathbb{E}_q [-\log w_{\theta^t}^{t+1}]$ constructed by the population predictive coding algorithm (Algorithm 1) has a*
 623 *pathwise derivative as the expectation of the negative gradient of the log-joint density*

$$\nabla_{\theta^t} \mathcal{F}^{t+1} = \mathbb{E}_q [-\nabla_{\theta^t} \log p_{\theta^t}(\mathbf{x}, \mathbf{z}^{t+1})].$$

624 *Proof.* The free energy has an expression in terms of Equation 8

$$\begin{aligned}\mathcal{F}^{t+1} &= \mathbb{E}_q [-\log w_{\theta^t}^{t+1}] & w_{\theta^t}^{t+1} &= \frac{p_{\theta^t}(\mathbf{x}, \mathbf{z})}{\prod_{z \in \mathbf{z}} \gamma_{\theta}(z_b^{t+1}; \mathbf{z}_{\setminus z})} \prod_{z \in \mathbf{z}} \hat{Z}_{\theta^t}(\mathbf{z}_{\setminus z})^{t+1}, \\ \hat{Z}_{\theta^t}(\mathbf{z}_{\setminus z})^{t+1} &= \frac{1}{K} \sum_{k=1}^K u_b^{t+1,k} & u_z^{t+1} &= \frac{\gamma_{\theta}(z^{t+1}; \mathbf{z}_{\setminus z})}{q(z^{t+1} | \varepsilon_z(z^t))},\end{aligned}$$

625 and writing out the free energy itself in full shows that many terms cancel

$$\begin{aligned}q(\mathbf{z}^{t+1} | \mathbf{z}^t) &= \prod_{z_b^{t+1} \in \mathbf{z}^{t+1}} q(z^{t+1} | z^t), \\ \mathcal{F}^{t+1} &= \mathbb{E}_{q(\mathbf{z}^{t+1} | \mathbf{z}^t)} \left[-\log \frac{p_{\theta^t}(\mathbf{x}, \mathbf{z})}{\prod_{z \in \mathbf{z}} \gamma_{\theta}(z_b^{t+1}; \mathbf{z}_{\setminus z})} \prod_{z \in \mathbf{z}} \frac{1}{K} \sum_{k=1}^K \frac{\gamma_{\theta}(z_b^{t+1}; \mathbf{z}_{\setminus z})}{q(z^{t+1} | \varepsilon_z(z^t))} \right] \\ &= \mathbb{E}_{q(\mathbf{z}^{t+1} | \mathbf{z}^t)} \left[-\log \frac{p_{\theta^t}(\mathbf{x}, \mathbf{z})}{\prod_{z \in \mathbf{z}} \gamma_{\theta}(z_b^{t+1}; \mathbf{z}_{\setminus z})} \frac{\prod_{z \in \mathbf{z}} \gamma_{\theta}(z_b^{t+1}; \mathbf{z}_{\setminus z})}{\prod_{z \in \mathbf{z}} q(z^{t+1} | \varepsilon_z(z^t))} \right] \\ &= \mathbb{E}_{q(\mathbf{z}^{t+1} | \mathbf{z}^t)} \left[-\log \frac{p_{\theta^t}(\mathbf{x}, \mathbf{z})}{q(\mathbf{z}^{t+1} | \mathbf{z}^t)} \right].\end{aligned}$$

626 The proposal distribution q is a function of the random variable values themselves through the
627 prediction errors, not of the parameters θ . The above expression therefore admits a pathwise
628 derivative [Schulman et al., 2015], moving the gradient operator into the expectation

$$\begin{aligned}\nabla_{\theta^t} \mathcal{F}^{t+1} &= \nabla_{\theta^t} \mathbb{E}_{q(\mathbf{z}^{t+1} | \mathbf{z}^t)} \left[-\log \frac{p_{\theta^t}(\mathbf{x}, \mathbf{z}^{t+1})}{q(\mathbf{z}^{t+1} | \mathbf{z}^t)} \right] \\ &= \mathbb{E}_{q(\mathbf{z}^{t+1} | \mathbf{z}^t)} \left[\nabla_{\theta^t} -\log \frac{p_{\theta^t}(\mathbf{x}, \mathbf{z}^{t+1})}{q(\mathbf{z}^{t+1} | \mathbf{z}^t)} \right] \\ &= \mathbb{E}_{q(\mathbf{z}^{t+1} | \mathbf{z}^t)} \left[\nabla_{\theta^t} - [\log p_{\theta^t}(\mathbf{x}, \mathbf{z}^{t+1}) - \log q(\mathbf{z}^{t+1} | \mathbf{z}^t)] \right] \\ &= \mathbb{E}_{q(\mathbf{z}^{t+1} | \mathbf{z}^t)} \left[-[\nabla_{\theta^t} \log p_{\theta^t}(\mathbf{x}, \mathbf{z}^{t+1}) - \nabla_{\theta^t} \log q(\mathbf{z}^{t+1} | \mathbf{z}^t)] \right] \\ \nabla_{\theta^t} \mathcal{F}^{t+1} &= \mathbb{E}_{q(\mathbf{z}^{t+1} | \mathbf{z}^t)} \left[-\nabla_{\theta^t} \log p_{\theta^t}(\mathbf{x}, \mathbf{z}^{t+1}) \right].\end{aligned}\quad \square$$

629 **Proposition 4** (DCPC coordinate updates are strictly properly weighted for the complete conditionals).
630 Each DCPC coordinate update (Equation 7) for a latent variable $z \in \mathbf{z}$ is strictly properly weighted
631 (Definition 2) for z 's unnormalized complete conditional. For every measurable $h : \mathcal{Z} \rightarrow \mathbb{R}$

$$\mathbb{E}_{z \sim q_{\eta}(z^t | z^{t-1}, \varepsilon_z^t)} \left[\mathbb{E}_{u \sim \delta(u), z', \hat{Z} \sim \text{RESAMPLE}(z, u_z)} [h(z)] \right] = \int_{z \in \mathcal{Z}} h(z) \gamma_{\theta}(z; \mathbf{z}_{\setminus z}) dz. \quad (13)$$

632 *Proof.* Expanding the outer expectation into an integral and replacing the Dirac delta with the
633 expression for the local weights transforms Equation 13 into

$$\begin{aligned}\int_{z \in \mathcal{Z}} \frac{\gamma_{\theta}(z; \mathbf{z}_{\setminus z})}{q_{\eta}(z | z^{t-1}, \varepsilon_z^t)} \mathbb{E}_{z' \sim \text{RESAMPLE}(z, u_z)} [h(z')] q_{\eta}(z | z^{t-1}, \varepsilon_z^t) dz &= \\ &= \int_{z \in \mathcal{Z}} h(z) \gamma_{\theta}(z; \mathbf{z}_{\setminus z}) dz;\end{aligned}$$

634 importance resampling also preserves strict proper weighting (see Naesseth et al. [2015], Stites et al.
635 [2021] and Chopin and Papaspiliopoulos [2020] for proofs), and so this yields

$$\begin{aligned}\int_{z \in \mathcal{Z}} \mathbb{E}_{z' \sim \text{RESAMPLE}(z, u_z)} [h(z')] \gamma_{\theta}(z; \mathbf{z}_{\setminus z}) dz &= \int_{z \in \mathcal{Z}} h(z) \gamma_{\theta}(z; \mathbf{z}_{\setminus z}) dz \\ \int_{z' \in \mathcal{Z}} h(z') \gamma_{\theta}(z'; \mathbf{z}_{\setminus z}) dz' &= \int_{z \in \mathcal{Z}} h(z) \gamma_{\theta}(z; \mathbf{z}_{\setminus z}) dz.\end{aligned}$$

636 \square

637 **Corollary 4.1** (DCPC coordinate updates sample from the true complete conditionals). *Each DCPC*
638 *coordinate update (Equation 7) for a latent $z \in \mathbf{z}$ samples from z 's complete conditional (the*
639 *normalization of Equation 5). Formally, for every measurable $h : \mathcal{Z} \rightarrow \mathbb{R}$, resampled expectations*
640 *with respect to the DCPC coordinate update equal those with respect to the complete conditional*

$$\mathbb{E}_{z \sim q_\eta(z|z^{t-1}, \varepsilon_z^t)} [\mathbb{E}_{u \sim \delta(u), z' \sim \text{RESAMPLE}(z, u_z)} [h(z')]] = \int_{z \in \mathcal{Z}} h(z) \pi_\theta(z | \mathbf{z}_{\setminus z}) dz.$$

641 *Proof.* Proposition 4 in Appendix B provides a lemma

$$\mathbb{E}_{z \sim q_\eta(z|z^{t-1}, \varepsilon_z^t)} [\mathbb{E}_{u \sim \delta(u), \hat{z} \sim \text{RESAMPLE}(z, u_z)} [h(z')]] = \int_{z \in \mathcal{Z}} h(z) \gamma_\theta(z; \mathbf{z}_{\setminus z}) dz,$$

642 which we can apply by observing that resampling sums over self-normalized weights

$$\begin{aligned} \mathbb{E}_{z \sim q_\eta(z|z^{t-1}, \varepsilon_z^t)} [\mathbb{E}_{u \sim \delta(u), z' \sim \text{RESAMPLE}(z, u_z)} [h(z)]] &= \\ &= \mathbb{E}_{z \sim q_\eta(z|z^{t-1}, \varepsilon_z^t)} \left[\mathbb{E}_{u \sim \delta(u)} \left[\mathbb{E}_{z' \sim \frac{u \delta_z(\cdot)}{\sum u'}} [h(z')] \right] \right], \end{aligned}$$

643 which is just a weighted sum that by Definition 2 is itself properly weighted

$$\begin{aligned} \mathbb{E}_{z \sim q_\eta(z|z^{t-1}, \varepsilon_z^t)} \left[\mathbb{E}_{u \sim \delta(u)} \left[\mathbb{E}_{z' \sim \frac{u \delta_z(\cdot)}{\sum u'}} [h(z')] \right] \right] &= \mathbb{E}_{z \sim q_\eta(z|z^{t-1}, \varepsilon_z^t)} \left[\mathbb{E}_{u \sim \delta(u)} \left[\frac{u}{\sum u} h(z) \right] \right] \\ &= \mathbb{E}_{z \sim q_\eta(z|z^{t-1}, \varepsilon_z^t)} \left[\mathbb{E}_{u \sim \delta(u)} \left[\frac{1}{\sum u} \int_{z \in \mathcal{Z}} h(z) \gamma_\theta(z; \mathbf{x}, \mathbf{z}_{\setminus z}) dz \right] \right] \\ &= \mathbb{E}_{z \sim q_\eta(z|z^{t-1}, \varepsilon_z^t)} \left[\mathbb{E}_{u \sim \delta(u)} \left[\frac{1}{\cancel{\hat{Z}_\theta(\mathbf{x}, \mathbf{z}_{\setminus z})} \cancel{Z_\theta(\mathbf{x}, \mathbf{z}_{\setminus z})}} \int_{z \in \mathcal{Z}} h(z) \pi_\theta(z | \mathbf{x}, \mathbf{z}_{\setminus z}) dz \right] \right] \\ &= \int_{z \in \mathcal{Z}} h(z) \pi_\theta(z | \mathbf{x}, \mathbf{z}_{\setminus z}) dz. \quad \square \end{aligned}$$

645 **Proposition 5** (DCPC parameter learning requires only local gradients in a factorized generative
646 model). *Consider a graphical model factorized according to Equation 1, with the additional assumption*
647 *that the model parameters $\theta \in \Theta = \prod_{x \in \mathbf{x}} \Theta_x \times \prod_{z \in \mathbf{z}} \Theta_z$ share that factorization. Then the*
648 *gradient $\nabla_\theta \mathcal{F}(\theta, q)$ of DCPC's free energy similarly factorizes into a sum of local particle averages*

$$\begin{aligned} \nabla_\theta \mathcal{F} &= \mathbb{E}_q [-\nabla_\theta \log p_\theta(\mathbf{x}, \mathbf{z})] \\ &= \sum_{v \in (\mathbf{x}, \mathbf{z})} \mathbb{E}_{q(v, \text{Pa}(v) | \varepsilon_v, \varepsilon_{\text{Pa}(v)})} [-\nabla_{\theta_v} \log p_{\theta_v}(v | \text{Pa}(v))] \\ &= - \sum_{v \in (\mathbf{x}, \mathbf{z})} \frac{1}{K} \sum_{k=1}^K \nabla_{\theta_v} \log p_{\theta_v}(v^k | \text{Pa}(v)^k). \end{aligned}$$

649 *Proof.* Proposition 3 provides the lemma that $\nabla_\theta \mathcal{F} = \mathbb{E}_q [-\nabla_\theta \log p_\theta(\mathbf{x}, \mathbf{z})]$, and applying the
650 factorization of the generative model demonstrates that

$$\nabla_\theta \mathcal{F} = \mathbb{E}_q \left[-\nabla_\theta \sum_{v \in (\mathbf{x}, \mathbf{z})} \log p_\theta(v | \text{Pa}(v)) \right].$$

651 Since the proposal q does not depend on any θ and consists of a particle cloud, we can rewrite it as a
652 mixture over the particles (after sampling is performed)

$$\nabla_\theta \mathcal{F} \approx \frac{1}{K} \sum_{k=1}^K -\nabla_\theta \sum_{v \in (\mathbf{x}, \mathbf{z})} \log p_\theta(v^k | \text{Pa}(v)^k),$$

653 and then finally apply the assumption of this theorem that $\theta \in \Theta = \prod_{x \in \mathbf{x}} \Theta_x \times \prod_{z \in \mathbf{z}} \Theta_z$, moving
654 the gradient operation into the sum over individual random variables

$$\approx \frac{1}{K} \sum_{k=1}^K \sum_{v \in (\mathbf{x}, \mathbf{z})} -\nabla_{\theta_v} \log p_{\theta_v}(v^k | \text{Pa}(v)^k). \quad \square$$

C Extension to discrete sample spaces

Contemporaneously to the work of Kuntz et al. [2023] on particle gradient descent, Sun et al. [2023] derived a novel Wasserstein gradient flow and corresponding descent algorithm for discrete distributions. In their setting, each Wasserstein gradient step constructs a D -dimensional, finitely supported distribution over the C -Hamming ball of the starting sample, such that the distribution has DC possible states in total. Let $z^{t+h} \in N_C(z^t)$ denote the resulting discrete random variable in the C -neighborhood around z^t with respect to the Hamming distance. The update rule relies on simulating the gradient flow for time h , sampling from a Markov jump process at time $t + h$

$$z^{t+h} \sim \prod_{d \in [1 \dots D]} q(z_d^{t+h} | z_d^t).$$

A rate matrix $Q_d(z^t)$ defined by the entire discrete variable z^t parameterizes the proposal distribution

$$q_h(z_d^{t+h} | z^t) = \exp(Q_d(z^t)h). \quad (14)$$

the rate matrix will have nondiagonal entries at indices $i \neq j \in [1 \dots C]$ in the neighborhood $N_C(z^t)$,

$$Q_d(z^t)_{i,j} = w_{i,j} g \left(\frac{\pi_\theta(z_{\setminus d}^t, z'_{d,j})}{\pi_\theta(z_{\setminus d}^t, z'_{d,i})} \right).$$

The above equation requires that $\forall i, j \in [1 \dots C], w_{i,j} = w_{j,i} \in \mathbb{R}$ and $g(a) = ag(\frac{1}{a})$. The ratio of normalized target densities π will equal the ratio of unnormalized densities γ

$$\frac{\pi_\theta(z_{\setminus d}^t, z'_{d,j})}{\pi_\theta(z_{\setminus d}^t, z'_{d,i})} = \frac{\gamma_\theta(z'_{d,j}; z_{\setminus d}^t) Z_{z_{\setminus d}^t}(z_{\setminus d}^t, \theta)}{Z_{z_{\setminus d}^t}(z_{\setminus d}^t) \gamma_\theta(z'_{d,i}; z_{\setminus d}^t)}$$

$$g \left(\frac{\pi_\theta(z_{\setminus d}^t, z'_{d,j})}{\pi_\theta(z_{\setminus d}^t, z'_{d,i})} \right) = g \left(\frac{\gamma_\theta(z'_{d,j}; z_{\setminus d}^t)}{\gamma_\theta(z'_{d,i}; z_{\setminus d}^t)} \right).$$

Based on the experimental recommendations of Sun et al. [2023], let $w_{i,j} = w_{j,i} = 1$ and $g(a) = \sqrt{a}$. The rate matrix then simplifies to nondiagonal and diagonal terms

$$Q_d(z^t)_{i,j} = \sqrt{\frac{\gamma_\theta(z'_{d,j}; z_{\setminus d}^t)}{\gamma_\theta(z'_{d,i}; z_{\setminus d}^t)}}, \quad Q_d(z^t)_{i,i} = - \sum_{j \neq i} Q_d(z^t)_{i,j}. \quad (15)$$

Equations 14 and 15 give a distribution descending the Wasserstein gradient of the free energy with respect to a particle cloud in a discrete sample space. Applying Equation 15 to $\gamma_\theta(z; \mathbf{z}_{\setminus z}^t)$ yields a factorization in log space

$$Q(z^t)_{i,j} = \sqrt{\frac{\gamma_\theta(z^t + i; \mathbf{z}_{\setminus z}^t)}{\gamma_\theta(z^t + j; \mathbf{z}_{\setminus z}^t)}} \log Q(z^t)_{i,j} = \frac{1}{2} \left(\log \gamma_\theta(z^t + i; \mathbf{z}_{\setminus z}^t) - \log \gamma_\theta(z^t + j; \mathbf{z}_{\setminus z}^t) \right).$$

This difference can be written as a difference of differences

$$\log \gamma_\theta(z^t + i; \mathbf{z}_{\setminus z}^t) - \log \gamma_\theta(z^t + j; \mathbf{z}_{\setminus z}^t) = \left(\log \gamma_\theta(z^t + i; \mathbf{z}_{\setminus z}^t) - \log \gamma_\theta(z^t; \mathbf{z}_{\setminus z}^t) \right) - \left(\log \gamma_\theta(z^t + j; \mathbf{z}_{\setminus z}^t) - \log \gamma_\theta(z^t; \mathbf{z}_{\setminus z}^t) \right). \quad (16)$$

Recent work on efficient sampling for discrete distributions has focused on approximating density ratios, such as the one in Equation 15, with series expansions parameterized by error vectors. When the underlying discrete densities consist of exponentiating a differentiable energy function, as in Grathwohl et al. [2021], these error vectors have taken the form of gradients and the finite-series expansions have been Taylor series. When they do not, Xiang et al. [2023] showed how they take the form of finite differences and Newton's series

$$\log \gamma(z') - \log \gamma(z) \approx \Delta_1 (\log \gamma(z))^\top \cdot (z' - z). \quad (17)$$

679 Discrete DCPC would therefore use finite differences as discrete prediction errors, breaking each
 680 discrete $z \in \mathbf{z}$ into dimensions and incrementing each dimension separately to construct a vector

$$\Delta_1 f(z) := (f(z_1 + 1, z_{2:D}), \dots, f(z_{1:i}, z_i + 1, z_{i+1:D}), \dots, f(z_{1:D-1}, z_D + 1)) \ominus f(z), \quad (18)$$

681 where \ominus subtracts the scalar $f(z)$ from the vector elements and $f : \mathbb{Z}^D \rightarrow \mathbb{R}$ is the target function.
 682 This would lead to defining the discrete prediction error as the finite difference

$$\varepsilon_z := \Delta_1 \log \gamma_\theta(z^t; \mathbf{z}_{\setminus z}^t). \quad (19)$$

683 Applying Equation 17 to the two terms of Equation 16, we obtain the approximations

$$\begin{aligned} \log \gamma_\theta(z^t + i; \mathbf{z}_{\setminus z}^t) - \log \gamma_\theta(z^t; \mathbf{z}_{\setminus z}^t) &\approx \Delta_1 \left(\log \gamma_\theta(z^t; \mathbf{z}_{\setminus z}^t) \right)^\top \cdot ((z^t + i) - z^t) \\ &\approx \varepsilon_z(z^t)^\top \cdot i \\ \log \gamma_\theta(z^t + j; \mathbf{z}_{\setminus z}^t) - \log \gamma_\theta(z^t; \mathbf{z}_{\setminus z}^t) &\approx \Delta_1 \left(\log \gamma_\theta(z^t; \mathbf{z}_{\setminus z}^t) \right)^\top \cdot ((z^t + j) - z^t) \\ &\approx \varepsilon_z(z^t)^\top \cdot j, \\ \log Q(z^t)_{i,j} &\approx \frac{1}{2} \varepsilon_z(z^t)^\top (i - j). \end{aligned}$$

684 Discrete DCPC would thus parameterize its discrete proposal (Equation 14) in terms of ε_z (Equa-
 685 tion 19), so that Equation 15 comes out to the (matrix) exponential of the (elementwise) exponential

$$q_h(z^{t+h} \mid \varepsilon_z) = \exp(Q(\varepsilon_z)h) \quad Q_d(\varepsilon_z)_{i,j} = \exp\left(\frac{(\varepsilon_z)_d^\top (i_d - j_d)}{2}\right).$$

Supplementary References

- Nicolas Chopin and Omiros Papaspiliopoulos. *An Introduction to Sequential Monte Carlo*. Springer, 2020. ISBN 978-3-030-47844-5. doi: 10.1007/978-3-030-47845-2. Citation Key: Chopin2020 ISSN: 2197-568X.
- Will Grathwohl, Kevin Swersky, Milad Hashemi, David Duvenaud, and Chris Maddison. Oops I took a gradient: Scalable sampling for discrete distributions. In *Proceedings of the 38th International Conference on Machine Learning*, page 3831–3841. PMLR, July 2021. URL <https://proceedings.mlr.press/v139/grathwohl21a.html>.
- John Schulman, Nicolas Heess, Theophane Weber, and Pieter Abbeel. Gradient estimation using stochastic computation graphs. In C. Cortes, N. Lawrence, D. Lee, M. Sugiyama, and R. Garnett, editors, *Advances in Neural Information Processing Systems*, volume 28. Curran Associates, Inc., 2015. URL https://proceedings.neurips.cc/paper_files/paper/2015/file/de03beffeed9da5f3639a621bcab5dd4-Paper.pdf.
- Haoran Sun, Hanjun Dai, Bo Dai, Haomin Zhou, and Dale Schuurmans. Discrete Langevin Samplers via Wasserstein Gradient Flow. In *Proceedings of the 26th International Conference on Artificial Intelligence and Statistics*, Valencia, Spain, April 2023. Proceedings of Machine Learning Research.
- Hao Wu, Heiko Zimmermann, Eli Sennesh, Tuan Anh Le, and Jan Willem van de Meent. Amortized population Gibbs samplers with neural sufficient statistics. In *Proceedings of the 37th International Conference on Machine Learning*, 2020.
- Yue Xiang, Dongyao Zhu, Bowen Lei, Dongkuan Xu, and Ruqi Zhang. Efficient Informed Proposals for Discrete Distributions via Newton’s Series Approximation. In *Proceedings of The 26th International Conference on Artificial Intelligence and Statistics*, pages 7288–7310. PMLR, April 2023. URL <https://proceedings.mlr.press/v206/xiang23a.html>. ISSN: 2640-3498.
- Heiko Zimmermann, Hao Wu, Babak Esmaeili, and Jan-Willem van de Meent. Nested variational inference. In M. Ranzato, A. Beygelzimer, Y. Dauphin, P.S. Liang, and J. Wortman Vaughan, editors, *Advances in Neural Information Processing Systems*, volume 34, pages 20423–20435. Curran Associates, Inc., 2021. URL https://proceedings.neurips.cc/paper_files/paper/2021/file/ab49b208848abe14418090d95df0d590-Paper.pdf.